IEEE Access
Multidisciplinary ⋮ Rapid Review ⋮ Open Access Journal

Received November 27, 2020, accepted December 13, 2020, date of publication December 22, 2020,
date of current version January 25, 2021.

Digital Object Identifier 10.1109/ACCESS.2020.3046517

Predictive Control of a Supercavitating Vehicle Based on Time-Delay Characteristics

YUNTAO HAN, ZHEN XU, AND LIANWU GUAN
College of Intelligent Systems Science and Engineering, Harbin Engineering University, Harbin 150001, China
Corresponding authors: Yuntao Han (yuntaohan@163.com) and Zhen Xu (2326044663@qq.com)

This work was supported in part by the National Natural Science Foundation of China under Grant 51209049, and in part by the Natural Science Foundation of Heilongjiang Province under Grant E2017015.

ABSTRACT Supercavitation technology can greatly improve the speed of underwater vehicles by reducing drag. However, the time-delay characteristic of a supercavitating vehicle presents control challenge. In this paper, a linear parameter-varying (LPV) time-delay model for a supercavitating vehicle is established by analysing the time-delay characteristics of the planing force. Moreover, considering that the cavitation radius is easily perturbed by external disturbances, a supercavitating LPV delay model depicted as a polytope is established. Based on the model, a predictive controller based on time-delay characteristics is designed. The controller can solve linear matrix inequalities (LMI) online to find the optimal solution at a given moment. In addition, the controller introduces a different Lyapunov function and multiple free control variables to reduce the system's conservativeness and expand the system's initial feasible region, which can improve the control performance of the system. A simulation verifies that the system exhibits good stability and robustness.

INDEX TERMS LMI, predictive controller, planing force, supercavitation, time-delay characteristics.

I. INTRODUCTION

Due to the Bernoulli effect, when the speed of an underwater vehicle reaches a certain range, supercavitation will arise on the surface of the vehicle. Unlike normal the cavitation, except for the fins and the tail, supercavitation will cover the whole vehicle. The reduction of contact area with the water leads to a significant reduction of the friction force during the forward movement of the vehicle. Because of its strong drag reduction effect, supercavitation technology has become a topic of interest in high-speed underwater vehicle researchs worldwide. However, the existence of supercavitation also creates severe nonlinear forces and exhibits systemic time-delay characteristics. Therefore, establishing an effective control strategy for these nonlinear forces and time-delay characteristics has great significance for the development of supercavitating technology.

A. DEVELOPMENT OF SUPERCAVITATING TECHNOLOGY

Currently, it is very difficult to model a supercavitating vehicle because of the existence of cavitation. In the middle of the last century, Ukraine and Russia started studying supercavitating vehicles. Logvinovich [1] determined the theory of independent expansion by studying the cavitation phenomenon of vehicles. In 1980, a formula for calculating the planing force [2] was established to determine the relationship between immersion depth and angle based on the supercavitating model studied by Wagner. In [3], the author summarized the research on memory effects and finally established a model of the time delay of supercavition. The relationship between the planing force of the supercavitating vehicle and the states at the previous moment was identified. Subsequently, scholars from different countries contributed numerous supercavitation theories and experimental studies based on the theory of the Bernoulli effect and the theory of independent expansion. In [4], a motion control model of a vehicle was proposed based on cavitation theory and considering the time-delay effect of supercavitation. The model was simplified as straight-and-level flight without roll. When a supercavitating vehicle turns, the model under the condition of straight line navigation is not suitable for this situation. Therefore, a mathematical model of a manoeuvrable supercavitating vehicle was established in [5]. In [6], the author developed a dive-plane model with noncylindrical and nonsymmetric cavity shapes instead of constant cylindrical cavities. In [7], the author proposed a general form

The associate editor coordinating the review of this manuscript and approving it for publication was Salman Ahmed.

of a pitch-plane model for supercavitating vehicle dynamics that considered vehicle motions into and out of the cavity, the unstable nature of the planing force and the memory effect. In [8], to maintain the stability of the supercavitating vehicle during the turn, a pair of elevators was used to achieve the functionality of the ailerons and roll damping was provided by a pair of rudders. Based on the result, a mathematical model of a supercavitating vehicle was designed. In [9], the author created an integrated dynamic model of a supercavitating vehicle, and constructed a 6-DOF equation of motion. In [10], the author proposed a spatial kinetics model for supercavitating vehicles that considered the coupled motions of pitch, yaw, and roll.

The control of the planing force has become a major challenge in supercavitating vehicle researchs. In [3], the author developed a control system based on feedback linearization for a high-speed supercavitating underwater vehicle. In [11], the author improved the control system and proposed a longitudinal trajectory tracking control system based on feedback linearization and receding horizon control. In [12], the author proposed a systematic approach to the parameter-dependent control synthesis of a high-speed supercavitation vehicle. A linear parameter-varying (LPV) controller was also synthesized for angle rate tracking in the presence of model uncertainty. In [13], the author developed a simplified supercavitation model. A continuous planing mode controller was designed for a supercavitating vehicle with parameter uncertainty, and the unknown upper limit of uncertainty was estimated by using adaptive technology. In [14], the author proposed a comprehensive framework for controllers to avoid planing force, and studied the trade-off between tracking performance and planing force avoidance. In [15], to ensure that the controller maintains stable control performance with modelling uncertainty, the author analysed and numerically studied the dynamic characteristics of a supercavitating vehicle in the transition phase from fully wetted to supercavitating operation, and proposed an adaptive control method based on neural networks. In [16], the main nonlinearity related to the planing force was considered in a supercavitation model. A linear quadratic regulator control scheme and a robust backstepping control scheme were proposed to achieve stable system dynamics and tracking response.

The time delay of the supercavitating vehicle is mainly the state delay caused by the memory effect and the input delay caused by the actuator. At present, there are few studies on the input time delay of supercavitating vehicles. In [17], an output feedback robust controller was proposed for a class of MIMO nonlinear systems with time-varying input delays and additive bounded disturbances. The focus of research on the time delay characteristics of supercavitation is mainly focused on the memory effec [18]. Most studies on the control of supercavitating vehicles have been based on nondelayed models. However, there are large differences between models with time delay and without time delay, so a controller designed for a model without time delay is not suitable for a model with time delay. In some references, a time-delay model of a supercavitating vehicle was adopted, but the time delay is considered as part of the disturbance. In [19], a model with a time delay was constructed and the physical basis of the delay effect was described. The time delay was approximately the length of the vehicle divided by its speed. It was found that open-loop systems with and without time delay were unstable, and the feedback control law of a stable system without time delay was invalid. Then, in [20], based on this study, the author combined the effect of cavitation rotation during forward motion and developed a pitch-plane model of a supercavitating vehicle. Moreover, the author further verified that the feedback control law of a stable system was invalid in the presence of time delay. To date, the research of the supercavitating memory effect has shown progress. In [21], inner-loop control technology based on dynamic inversion was proposed to address the switched and delay-dependent behaviours of a supercavitating vehicle. Linear time-varying(LPV) technology [22] can effectively solve the problem of time delay. In [23], the cavitation memory effect was considered, and a supercavitating vehicle was modelled as a time-delay LPV system. Then, a powerful controller was designed to address the switched and delay-dependent behaviours of the vehicle. In [24], the physical basis of the convection delay and the expressions used to determine the immersion depth and immersion angle of the vehicle were given. An analysis and simulation of the time delay and unsteady planing system were carried out. In [25], a nonlinear time-delay dynamic model was established to design a complex control system for a supercavitating vehicle. Feedforward regulator and feedback regulator were designed respectively. Feedforward regulator was used to eliminate the interference of the planing force. In [26], the time delay gauss pseudospectral method (TDGPM) was developed to achieve fast optimization. By transforming the optimal control problem into a nonlinear programming (NLP) problem, the solution process was greatly accelerated. LMI is an important tool to solve the problem of time delay, among which there are important applications in maglev vehicles [27] and power electronics [28]. In [29], the authors applied LMI to solve the problem of parameter perturbation and time delay of the supercavitating vehicle. In [30], a vertical plane model with a time delay effect was developed. A new PID control algorithm with up and down rudder modes was designed based on a stability analysis of a pitch planing model related to delay. In [20], feedback control was designed by considering the time delay. The effectiveness of the controller was proven by a numerical study of a nonlinear delay-dependent pitch-plane model of supercavitating vehicle.

B. MAIN RESEARCH CONTENTS

Compared with other controllers [31], the controller designed in this paper can solve the optimal control law in each sampling period and improve the dynamic performance of

supercavitating vehicle. At the same time, the perturbation problem of the system cavity radius is considered in this paper, so that the supercavitating vehicle can remain stable when the cavity radius perturbation occurs. Moreover, the controller is improved to deal with the time delay problem of supercavitation effectively.

In this paper, the main innovations of this paper are: (i) How to deal with the time delay is the main problem in the controller design because the theory of independent expansion is considered. An LPV time-delay model of a supercavitating vehicle is established by decomposing and transforming the planing force to deal with the problem of time delay. (ii) Considering the variation in supercavitation fin motion and the variation in cavitation radius caused by the variation in fluid pressure on the surface of the cavitation wall, the model parameters are further modified. (iii) To improve the dynamic performance of the system, different Lyapunov function and a predictive control method with multiple free control variables are used. The controller in this paper can solve linear matrix inequalities (LMI) based on the state variables and delay variables of the system to obtain the optimal state feedback control law with memory feedback, which exhibits better control performance.

The organizational structure of this paper is as follows: In section II, the time-delay model of a supercavitating vehicle is briefly introduced, and an LPV time-delay model of supercavitating vehicle is constructed by decomposing the planing force. In section III, a predictive controller is designed. The simulation results are provided in section IV, and the conclusion is shown in section V.

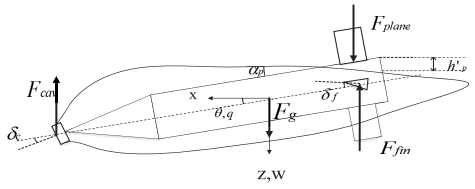

FIGURE 1. Supercavitating vehicle model.

II. SUPERCAVITATING VEHICLE MODELS

The Fig.1 shows the supercavitating vehicle model. Due to the existence of supercavitation, the forces on its longitudinal plane are composed of the force of the cavitator F_{cav}, the force of the fins F_{fin}, the planing force of the tail F_{plane} and the gravity of the vehicle F_g [32]. The resultant force in the vertical direction is:

$$F_{cav} + F_{fin} + F_{plane} + F_g = m_b(\dot{w} - x_g\dot{q} - qV) \tag{1}$$

where V is the forward velocity of the vehicle, m_b is the weight of the vehicle, x_g denotes the centre of gravity, w is the longitudinal velocity, q is the pitch angle velocity.

The following models can be established for the dynamics and kinematics analysis of the vehicle:

$$\begin{aligned} M_0\begin{bmatrix}\frac{dw}{dt}\\ \frac{dq}{dt}\end{bmatrix} &= A_0\begin{bmatrix}w\\ q\end{bmatrix} + B_0\begin{bmatrix}\delta_f\\ \delta_c\end{bmatrix} + F_g + F_{plane}\hat{}\begin{bmatrix}1\\ L\end{bmatrix}\\ \frac{dz}{dt} &= w - V\theta\\ \frac{d\theta}{dt} &= q \end{aligned} \tag{2}$$

$F_{plane}\hat{}$ is the normalized value of the planing force:

$$F_{plane}\hat{} = \frac{F_{plane}}{\pi\rho m R^2 L}$$

z is the depth of the vehicle, R represents the vehicle radius, θ is the pitch angle, δ_c represents the cavitation deflection angle, δ_f denotes the fins deflection angle, L is the length of the vehicle, m is the density ratio of the vehicle and the fluid, ρ represents the density of water, where

$$M_0 = \begin{bmatrix}\frac{7}{9} & \frac{16L}{16}\\ \frac{17L}{36} & \frac{11}{16}R^2 + \frac{133}{405}L^2\end{bmatrix}$$

$$A_0 = CV\begin{bmatrix}\frac{1+n}{m} & \frac{-n}{m}\\ \frac{-n}{m} & \frac{-nL}{m}\end{bmatrix}$$

$$B_0 = CV^2\begin{bmatrix}\frac{-n}{mL} & \frac{-1}{mL}\\ \frac{-n}{m} & 0\end{bmatrix} \quad F_g = \begin{bmatrix}\frac{7}{9}\\ \frac{17L}{36}\end{bmatrix} g$$

g is the acceleration of gravity and n denotes the effectiveness coefficient of the fins rudder. C can be defined as :

$$C = 0.5C_{x0}(1+\sigma)(\frac{R_n}{R})^2$$

R_n is the cavitator radius, C_{x0} is the lift coefficient, and σ denotes the cavitation number.

In [19] and [20], it was verified that there was a large difference between the response speed and tail swing frequency when a time-delay model and a non-delayed model were stable, so the controller design considering the time-delay is more important for the actual system. The planing force model of the supercavitating vehicle is:

$$F_{plane} = -\pi\rho R^2 V^2(\frac{1+h'_p}{1+2h'_p})(1-(\frac{R'}{R'+h'_p})^2)\alpha_p \tag{3}$$

where,

$$h'_p = \begin{cases}\dfrac{z(t)+\theta(t)L-z(t-\tau)+R-R_c}{R}, & \textit{bottom contact}\\ 0 & \textit{inside cavity}\\ \dfrac{R-R_c-z(t)-\theta(t)L+z(t-\tau)}{R}, & \textit{top contact}\end{cases}$$

$$\alpha_p = \begin{cases} \dfrac{\theta(t)-\theta(t-\tau)+[w(t-\tau)-\dot{R}_c]}{V}, & \textit{bottom contact} \\ 0 & \textit{inside cavity} \\ \dfrac{\theta(t)-\theta(t-\tau)+[w(t-\tau)+\dot{R}_c]}{V}, & \textit{top contact} \end{cases}$$
$$R' = (R_c - R)/R$$

h'_p represents immersion depth, α_p denotes immersion angle, $\tau = L/V$ is the size of time delay, R_c is cavitation radius, $\dot{R}_c$ denotes the contraction rate of the cavity at the planing location, where

$$R_c = R_n[0.82\frac{1+\sigma}{\sigma}]^{1/2}K_2,\ K_1 = \frac{L}{R_n}(\frac{1.92}{\sigma}-3)^{-1}-1$$
$$K_2 = [1-(1-\frac{4.5\sigma}{1+\sigma})K_1^{40/17}]^{1/2}$$
$$\dot{R}_c = -\frac{20}{17}\frac{(0.82\frac{1+\sigma}{\sigma})^{1/2}V((1-\frac{4.5\sigma}{1+\sigma})K_1^{23/17})}{K_2(\frac{1.92}{\sigma}-3)}$$

The conditions for the collision of the vehicle with the cavity wall are as follow:

$$\begin{cases} \textit{bottom contact} & \textit{if } R_c - R < z(t) + \theta(t)L - z(t-\tau) \\ \textit{inside cavity} & \textit{otherwise} \\ \textit{top contact} & \textit{if } R - R_c > z(t) + \theta(t)L - z(t-\tau) \end{cases} \tag{4}$$

Considering the planing force is nonlinear force, we define:

$$\gamma_1 = (\frac{1+h'_p}{1+2h'_p})(1-(\frac{R'}{R'+h'_p})^2)$$
$$\gamma_2 = \begin{cases} -\dot{R}_c/V, & \textit{bottom contact} \\ 0 & \textit{inside cavity} \\ \dot{R}_c/V, & \textit{top contact} \end{cases}$$
$$\gamma_3 = z(t) + \theta(t)L - z(t-\tau) \tag{5}$$

and define variables according to (5):

$$\pi_1 = \frac{V^2}{mL}\gamma_1 \quad \pi_2 = \frac{\gamma_2}{\gamma_3} \quad \pi_3 = \pi_1\pi_2 \tag{6}$$

According to [29], when the supercavitating vehicle has planing force, $\hat{F_{plane}}$ can be decomposed as follows:

$$\begin{aligned} \hat{F_{plane}} &= -\frac{V^2}{mL}(\frac{1+h'_p}{1+2h'_p})(1-(\frac{R'}{R'+h'_p})^2)\alpha_p \\ &= -\pi_1[\theta(t)-\theta(t-\tau)+w(t-\tau)/V+\gamma_2] \\ &= -\pi_1[\theta(t)-\theta(t-\tau)+w(t-\tau)/V] \\ &\quad -\pi_3[z(t)+\theta(t)L-z(t-\tau)] \\ &= \begin{bmatrix} -\pi_3 \\ 0 \\ -\pi_3L-\pi_1 \\ 0 \end{bmatrix}^T \begin{bmatrix} z(t) \\ w(t) \\ \theta(t) \\ q(t) \end{bmatrix} \\ &\quad + \begin{bmatrix} \pi_3 \\ -\pi_1/V \\ \pi_1 \\ 0 \end{bmatrix}^T \begin{bmatrix} z(t-\tau) \\ w(t-\tau) \\ \theta(t-\tau) \\ q(t-\tau) \end{bmatrix} \end{aligned} \tag{7}$$

We can get that from (7):

$$\begin{aligned} &\hat{F_{plane}}\begin{bmatrix} 1 \\ L \end{bmatrix} \\ &= \begin{bmatrix} -\pi_3 z(t) + (-\pi_1 - \pi_3 L)\theta(t) \\ -\pi_3 L z(t) + (-\pi_1 - \pi_3 L)L\theta(t) \end{bmatrix} \\ &\quad + \begin{bmatrix} \pi_3 z(t-\tau) - \frac{\pi_1}{V}w(t-\tau) + \pi_1\theta(t-\tau) \\ \pi_3 L z(t-\tau) - \frac{\pi_1}{V}Lw(t-\tau) + \pi_1 L\theta(t-\tau) \end{bmatrix} \\ &= \begin{bmatrix} -\pi_3 & -\pi_1 - \pi_3 L \\ -\pi_3 L & (-\pi_1 - \pi_3 L)L \end{bmatrix} \begin{bmatrix} z(t) \\ \theta(t) \end{bmatrix} \\ &\quad + \begin{bmatrix} \pi_3 & -\frac{\pi_1}{V} & \pi_1 \\ \pi_3 L & -\frac{\pi_1}{V}L & \pi_1 L \end{bmatrix} \begin{bmatrix} z(t-\tau) \\ w(t-\tau) \\ \theta(t-\tau) \end{bmatrix} \end{aligned} \tag{8}$$

(2) can be given in the following form:

$$M_0\begin{bmatrix} \frac{dw}{dt} \\ \frac{dq}{dt} \end{bmatrix} = A_0\begin{bmatrix} w \\ q \end{bmatrix} + B_0\begin{bmatrix} \delta_f \\ \delta_c \end{bmatrix} + F_g + C_0\begin{bmatrix} z \\ \theta \end{bmatrix} + D_0\begin{bmatrix} z_\tau \\ w_\tau \\ \theta_\tau \end{bmatrix}$$
$$\frac{dz}{dt} = w - V\theta$$
$$\frac{d\theta}{dt} = q \tag{9}$$

where, z_τ, w_τ, θ_τ are the state variables before τs.

$$C_0 = \begin{bmatrix} -\pi_3 & -\pi_1 - \pi_3 L \\ -\pi_3 L & -\pi_1 L - \pi_3 L^2 \end{bmatrix}$$
$$D_0 = \begin{bmatrix} \pi_3 & -\pi_1/V & \pi_1 \\ \pi_3 L & -\pi_1 L/V & \pi_1 L \end{bmatrix}$$

According to (9), we can obtain LPV delay model of supercavitating vehicle by linearizing the nonlinear planing force. According to the principle of independent expansion, the parameters related to the time delay are the system state of the cavitator passing through the section (when the planing force is generated).

$$\dot{x(t)} = A(\pi_1, \pi_3)x(t) + A_d(\pi_1, \pi_3)x(t-\tau) + Bu + G \tag{10}$$

If the time is t and the time delay is τ, the state variables where $x(t-\tau) = [z(t-\tau)\ w(t-\tau)\ \theta(t-\tau)\ q(t-\tau)]^T$ represents the state variable with delay of τ, $x(t) = [z(t)\ w(t)\ \theta(t)\ q(t)]^T$ is the state variable and $u = [\delta_f\ \delta_c]^T$ is control variable. B, C, G are constant matrices, $A(\pi_1, \pi_3)$ and $A_d(\pi_1, \pi_3)$ are time-varying matrices with π_1 and π_3 parameters. where,

$$A = \begin{bmatrix} 0 & 1 & -75 & 0 \\ 4.41\pi_1 & 15.30 & 4.41(\pi_1+1.8\pi_3) & 79.94 \\ 0 & 0 & 0 & 1 \\ -5.52\pi_1 & -13.27 & -5.52(\pi_1+1.8\pi_3) & 0 \end{bmatrix}$$
$$A_d = \begin{bmatrix} 0 & 0 & 0 & 0 \\ -4.41\pi_3 & -4.41\pi_1 & 0.0589\pi_1 & 0 \\ 0 & 0 & 0 & 0 \\ 5.52\pi_3 & 5.52\pi_1 & -0.0696\pi_1 & 0 \end{bmatrix}$$
$$B = \begin{bmatrix} 0 & 0 \\ 205.95 & 941.84 \\ 0 & 0 \\ -243.31 & 752.08 \end{bmatrix} \quad G = \begin{bmatrix} 0 \\ 9.81 \\ 0 \\ 0 \end{bmatrix}$$

TABLE 1. System parameters for simulations.

Parameter	Value
g	$9.81m/s^2$
m	2
n	0.5
R_n	$0.0191m$
R	$0.0508m$
R_c	0.0902
$\hat{R}_c$	-3.2965
L	1.8 m
V	$75m/s$
σ	0.03
C_{x0}	0.82

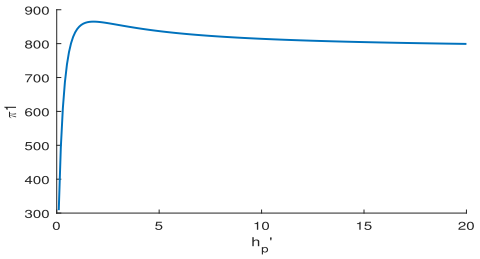

FIGURE 2. Change curve of π_1 with immersion depth h'_p.

III. PREDICTIVE CONTROL BASED ON FREE CONTROL VARIABLES

The variable parameters of LPV time-delay model are π_1 and π_3. According to (6), it can be seen that :

$$\lim_{h'_p \to \infty} \pi_1 = \frac{V^2}{mL} \tag{11}$$

And π_1 is greater than or equal to zero. Therefore, the relationship between π_1 and h'_p is shown in Fig.2. It can be seen from the Fig.2 that $\pi_1 \in [0, 865.625]$. According to (6), we know that:

$$0 \le \pi_2 = \begin{cases} -\dfrac{\dot{R}_c}{V(z(t)+\theta(t)L-z(t-\tau))}, & \textit{bottom contact} \\ 0 & \textit{inside cavity} \\ \dfrac{\dot{R}_c}{V(z(t)+\theta(t)L-z(t-\tau))}, & \textit{top contact} \end{cases}$$

When the vehicle collides with the lower wall of the cavity, $0 < R_c - R < z(t) + \theta(t) L - z(t-\tau)$. When the vehicle collides with the upper wall of the cavity, $0 > R - R_c > z(t) + \theta(t) L - z(t-\tau)$. We can get:

$$0 \le \pi_2 \le -\frac{\dot{R}_c}{V(R_c - R)} \tag{12}$$

And when R_c changes rapidly due to the change of the fins motion form or the change of the fluid pressure on the cavity wall at the fins rudder, the range of π_2 will change correspondingly. Because of $\pi_3 = \pi_1\pi_2$, the value of π_3 will also change. When the perturbation of cavitation radius is $\pm 20\%$, the relation curve between π_2 and γ_3 is as shown in Fig.3. Considering the perturbation of cavitation, we get $\pi_3 \in [0, 1416.35]$.

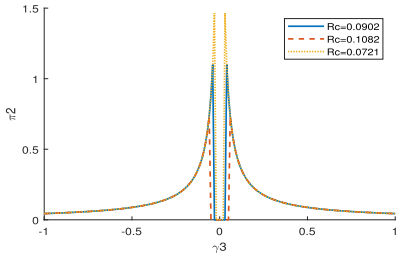

FIGURE 3. Change curve of π_2 with immersion depth γ_3.

This paper focuses on the influence of time delay on supercavitating vehicle, which is mainly related to planing force. When the system state and time delay state satisfy $R_c - R < z(t) + \theta(t) L - z(t-\tau)$, the planing force appears and the system collides with the cavity wall. When the system state is $R - R_c > z(t) + \theta(t) L - z(t-\tau)$, the system is in contact with the upper wall of the cavity. In other states, the vehicle is in the cavity, and the system has no planning force. When the vehicle meets the condition of planing force impacting the cavity wall, the immersion depth and angle of the system are no longer zero. it can be seen π_1 and π_3 are no longer zero from (5) (6). The time-varying parameters in this paper are π_1 and π_3. It can be seen from (7) that when π_1 and π_3 are equal to zero, the vehicle is inside the cavity and the system has no planing force. When π_1 and π_3 are not equal to zero, the system appears planing force. According to the [20], the planing force with time delay will make the system easier to diverge and make the system oscillate, which makes the control more difficult.

According to [33], the time-delay system of the supercavitating vehicle with (10) can be described by the following discrete linear time-varying model:

$$\begin{aligned} x(k+1) &= Ax(k) + A_d x(k-d) + Bu \quad [A\ A_d] \in \Omega \\ \Omega &= Co[A_1\ A_{d1}]\,[A_2\ A_{d2}] \cdots [A_i\ A_{di}] \end{aligned} \tag{13}$$

where $i = 4$. $[A_1\ A_{d1}]\ [A_2\ A_{d2}] \cdots [A_4\ A_{d4}]$ are the values of $A(\pi_1, \pi_3)$ and $A_d(\pi_1, \pi_3)$ when $[\pi_1\ \pi_3] = [0\ 0]\ [0\ 1416.35]\ [865.625\ 0]\ [865.625\ 1416.35]$. In the equation, Co is the convex hull sign, that is to say, for the time-varying matrices $A(\pi_1, \pi_3)$ and $A_d(\pi_1, \pi_3)$, the above formula indicates that there is a set of non-negative real numbers η_i satisfy:

$$[A(k)\ A_d(k)] = \sum_{i=1}^{4} \eta_i [A_i\ A_{di}],\ \sum_{i=1}^{4} \eta_i = 1,\ \eta_i \ge 0 \tag{14}$$

No matter how $A(k)$, $A_d(k)$ change, it will eventually fall into the convex hull Ω with $[A_i\ A_{di}]$ as the vertex. This representation method is called linear time-varying uncertain system described by polytope.

To expand the initial feasible region of the system, free control variables can be introduced into the infinite time domain. Knowing the state quantities at time k are $x(k|k) = x(k)$ and $x(k-d|k) = x(k-d)$, the state space prediction model of

the supercavitation system can be derived according to (10) as follows:

$$\begin{bmatrix} X(k) \\ x(k+N) \end{bmatrix} = \begin{bmatrix} G \\ \hat{G} \end{bmatrix} x(k) + \begin{bmatrix} K \\ \hat{K} \end{bmatrix} X_d(k) + \begin{bmatrix} M \\ \hat{M} \end{bmatrix} U(k) \quad (15)$$

where

$$X(k) = \begin{bmatrix} x(k+1) \\ x(k+2) \\ \vdots \\ x(k+N-1) \end{bmatrix} \quad U(k) = \begin{bmatrix} u(k) \\ u(k+1) \\ \vdots \\ u(k+N-1) \end{bmatrix}$$

$$X_d(k) = \begin{bmatrix} x(k-N) \\ x(k-N+1) \\ \vdots \\ x(k-1) \end{bmatrix} \quad G = \begin{bmatrix} A(k) = G(1) \\ A^1(k) = G(2) \\ \vdots \\ A^{N-2}(k) = G(N-1) \end{bmatrix}$$

$$K = \begin{bmatrix} A_d(k) & 0 & \dots & 0 & 0 \\ A(k)A_d(k) & A_d(k) & \dots & 0 & 0 \\ \vdots & \vdots & \ddots & \vdots & \vdots \\ A^{N-3}(k)A_d(k) & A^{N-4}(k)A_d(k) & \dots & 0 & 0 \\ A^{N-2}(k)A_d(k) & A^{N-3}(k)A_d(k) & \dots & A_d(k) & 0 \end{bmatrix} = \begin{bmatrix} K(1) \\ K(2) \\ \vdots \\ K(N-1) \end{bmatrix}$$

$$M = \begin{bmatrix} B & 0 & \dots & 0 & 0 \\ A(k)B & B & \dots & 0 & 0 \\ \vdots & \vdots & \ddots & \vdots & \vdots \\ A^{N-3}(k)B & A^{N-4}(k)B & \dots & 0 & 0 \\ A^{N-2}(k)B & A^{N-3}(k)B & \dots & B & 0 \end{bmatrix} = \begin{bmatrix} M(1) \\ M(2) \\ \vdots \\ M(N-1) \end{bmatrix}$$

$$\hat{K} = \begin{bmatrix} A^{N-1}(k)A_d(k) & A^{N-2}(k)A_d(k) & \dots & A_d(k) \end{bmatrix}$$

$$\hat{G} = A^{N-1}\ \hat{M} = \begin{bmatrix} A^{N-1}(k)B & A^{N-2}(k)B & \dots & B \end{bmatrix}$$

$U(k)$ represents the matrix composed of the first free control variables used. In the first $N-1$ steps of the system, free control variables are used to introduce the system into the control invariant set, and then the following fixed state feedback law [34] is used:

$$u(k+i|k) = K_1(k)x(i+i|k) + K_2(k)x(k+i-d|k), \quad i \geq N \quad (16)$$

The stability of the system is achieved by the control law.

The predictive control of the supercavitating LPV model based on free control variables designed in this section can be expressed as the following min-max optimal solution problem:

$$\begin{aligned} &\min_{u(k+i|k), i\geq 0} \max_{[A(k)\ A_d(k)]\in\Omega} J_\infty \\ &\quad = \sum_{i=0}^{\infty} [||x(k+i|k)||_{\overline{Q}} + ||u(k+i|k)||_{\overline{R}}] \\ &\quad s.t\ x(k+i+1) = A(k)x(k+i|k) + A_d(k)x(k+i-d|k) \\ &\qquad + Bu(k+i|k),\ k>0, \quad i \geq 0 \\ &\qquad x(k|k) = x(k) \end{aligned} \quad (17)$$

This formula can be understood as the worst-case infinite time domain performance index that makes the parameter variate within Ω when performing rolling optimization. For the following multivariate Lyapunov functions:

$$\begin{aligned} &V(x(k+i|k)) \\ &\quad = x^T(k+i|k)P(i,k)x(k+i|k) \\ &\qquad + \sum_{j=1}^{d} x^T(k+i-j|k)P_d(i,k)x(k+i-j|k) \end{aligned} \quad (18)$$

where, $P(i,k)$ and $P_d(i,k)$ are symmetric positive definite matrix. According to [35], at k time, the fixed Lyapunov functions keep the matrices P and P_d constant, so the corresponding ellipse invariant sets remain unchanged. Therefore, the fixed Lyapunov functions limit the size of the ellipse invariant sets, which causes the predicted value of the system to be limited to a fixed ellipse invariant set. The variable Lyapunov functions break the limitation and change the ellipse invariant sets according to the change of the predicted states, which increases the degree of freedom and reduces the conservatism of the controller design. According to the properties of the polytope model, the time-varying term can be transformed as follows:

$$\begin{aligned} &P(i,k) = \eta_j(i,k)\sum_{j=1}^{4} P_j, \ \sum_{j=1}^{4}\eta_j(i,k) = 1, \quad \eta_j(i,k) \geq 0 \\ &P_d(i,k) = \eta_j(i,k)\sum_{j=1}^{4} P_{dj}, \ \sum_{j=1}^{4}\eta_j(i,k) = 1, \quad \eta_j(,k) \geq 0 \end{aligned} \quad (19)$$

Because $\eta(i,k)$ and $\eta(i+1,k)$ are not equal in the formula, $P(i,k)$, $P_d(i,k)$ are not equal to $P(i+1,k)$, $P_d(i+1,k)$.

For any $x(k)$ and $u(k)$, make their V-function satisfy:

$$\begin{aligned} &V(x(k+i+1|k)) - V(x(k+i|k)) \\ &\qquad \leq -[||x(k+i|k)||_{\overline{Q}} + ||u(k+i|k)||_{\overline{R}}] \end{aligned} \quad (20)$$

The following inequalities can be obtained by accumulating the expression from zero to infinity:

$$-V(x(k|k)) \leq -J_\infty \quad (21)$$

From this, the upper bound of the maximum performance problem can be acquired

$$\max_{[A(k)\ A_d(k)]\in\Omega} J_\infty \leq V(x(k|k)) \quad (22)$$

From (18) (21) (22), we can get:

$$\begin{aligned} &\max_{[A(k)\ A_d(k)]\in\Omega} J_\infty \leq J_N(k) \\ &\quad = \sum_{i=0}^{N-1} [||x(k+i|k)||_{\overline{Q}} + ||u(k+i|k)||_{\overline{R}}] + V(k+N|k) \end{aligned} \quad (23)$$

After the above processing, the online optimal problem in infinite time domain is transformed into the minimization problem in finite time domain with terminal constraints.

According to (18), the performance index can be changed as follows:

$$\begin{aligned} J_N(k) = &[||x(k)||_{\overline{Q}} + ||X(k)||_{\overline{Q}} + ||U(k+i|k)||_{\overline{R}}] \\ &+ ||x(k+N|k)||_{P(N,k)} \\ &+ \sum_{j=1}^{d} ||x(k+N-j|k)||_{P_d(N,k)} \end{aligned} \tag{24}$$

The number of prediction steps N is set to $N = \tau/T$, that is to say, the number of prediction steps is equal to the number of delay steps. The above formula can be written as:

$$\begin{aligned} &J_N(k) \\ &= [||x(k)||_{\overline{Q}} + ||X(k)||_{\overline{Q}} + ||U(k+i|k)||_{\overline{R}}] \\ &\quad + ||x(k+N|k)||_{P(N,k)} + ||x(k)||_{P_d(N,k)} \\ &\quad + \sum_{j=1}^{d-1} ||x(k+j|k)||_{P_d(N,k)} \\ &= [||x(k)||_{\overline{Q}} + ||Gx(k) + KX_d(k) + MU(k)||_{\overline{Q}} \\ &\quad + ||U(k+i|k)||_{\overline{R}}] + ||\hat{G}x(k) + \hat{K}X_d(k) + \hat{M}U(k)||_{P(N,k)} \\ &\quad + ||x(k)||_{P_d(N,k)} + ||Gx(k) + KX_d(k) + MU(k)||_{\hat{P}_d(N,k)} \\ &\le ||x(k)||_{\overline{Q}} + \lambda_1 + \lambda_2 \end{aligned} \tag{25}$$

where,

$$\begin{aligned} \lambda_1 &\ge ||Gx(k) + KX_d(k) + MU(k)||_{\overline{Q}} + ||U(k)||_{\overline{R}} \\ \lambda_2 &\ge ||x(k)||_{P_d(0,k)} + ||\hat{G}x(k) + \hat{K}X_d(k) \\ &\quad + \hat{M}U(k)||_{P(N,k)} + ||Gx(k) + KX_d(k) + MU(k)||_{\hat{P}_d(N,k)} \\ &\hat{P}_d(N,k) \\ &= \begin{bmatrix} P_d(N,k) & \dots & 0 \\ \vdots & \ddots & \vdots \\ 0 & \dots & P_d(N|k) \end{bmatrix} \end{aligned} \tag{26}$$

According to (26), if $P(i,k) = \lambda_2 Q^{-1}(i,k)$ and $P_d(i,k) = \lambda_2 K_d^{-1}(i,k)$, the time-varying matrix parameters of the system can be changed as follows :

$$\begin{bmatrix} \overline{Q}^{-1} & 0 & G_i x(k) + K_i X_d(k) + M_i U(k) \\ * & \overline{R}^{-1} & U(k) \\ * & * & \lambda_1 \end{bmatrix} \ge 0 \tag{27}$$

where $i = 1, 2 \dots l,\ l = 4$ represents the number of vertices of the polytope model. Similarly, the second Equation of (26) can be converted into the following LMI form:

$$\begin{bmatrix} 1 & \Theta^T & x^T(k) & \Theta_1^T & \dots & \Theta_{d-1}^T \\ * & Q_i & 0 & 0 & \dots & 0 \\ * & * & K_{di} & 0 & \dots & 0 \\ * & * & * & K_{di} & \dots & 0 \\ * & * & * & * & \ddots & \vdots \\ * & * & * & * & \dots & K_{di} \end{bmatrix} \ge 0 \tag{28}$$

where,

$$\begin{aligned} \Theta &= \hat{G}x(k) + \hat{K}X_d(k) + \hat{M}U(k) \\ \Theta_1 &= G(1)x(k) + K(1)X_d(k) + M(1)U(k) \\ \Theta_2 &= G(2)x(k) + K(2)X_d(k) + M(2)U(k) \\ \Theta_{d-1} &= G(d-1)x(k) + K(d-1)X_d(k) + M(d-1)U(k) \end{aligned}$$

Theorem 1: For the system shown in (13), the unknown matrices Q_i and K_{di} make the system asymptotically stable if the following condition are satisfied:

$$\begin{bmatrix} \Phi_1 & 0 & \Phi_2 & Y_1^T \overline{R}^{1/2} & E_1^T \overline{Q}^{1/2} & E_1^T \\ * & \Phi_3 & \Phi_4 & Y_2^T \overline{R}^{1/2} & 0 & 0 \\ * & * & Q_i & 0 & 0 & 0 \\ * & * & * & \lambda_2 I & 0 & 0 \\ * & * & * & * & \lambda_2 I & 0 \\ * & * & * & * & * & K_{di} \end{bmatrix} \ge 0$$

$$\Phi_1 = E_1 + E_1^T - Q_i,\ \Phi_2 = (A_i E_1 + B Y_1)^T$$

$$\Phi_3 = E_2 + E_2^T - K_{di},\ \Phi_4 = (A_{di} E_2 + B Y_2)^T$$

where $i = 1 \dots 4$, E_1 and E_2 are unknown invertible matrices, Y_1, Q_i, K_{di} and Y_2 are unknown matrices, $\overline{R}$ and $\overline{Q}$ are known matrices, λ_2 is unknown parameter.

Proof: To guarantee the asymptotically stable condition of the system, $V(k+i|k)$ at time k must be forced to decrease continuously, that is:

$$\begin{aligned} &V(x(k+i+1|k)) - V(x(k+i|k)) \\ &\qquad \le -[||x(k+i|k)||_{\overline{Q}} + ||u(k+i|k)||_{\overline{R}}] \end{aligned}$$

where $i \ge N$. After introducing state feedback, the equation can be decomposed into the following form:

$$\begin{bmatrix} x(k+i|k) \\ x(k+i-d|k) \end{bmatrix}^T \begin{bmatrix} \phi_1 & \phi_2 \\ \phi_3 & \phi_4 \end{bmatrix} \begin{bmatrix} x(k+i|k) \\ x(k+i-d|k) \le 0 \end{bmatrix}$$

$$\begin{aligned} \phi_1 &= \lambda_2(k)[||A(k) + BK_1||_{Q^{-1}(i+1,k)} + K_d(i+1,k) \\ &\quad - Q^{-1}(i,k)] + \overline{Q} + K_1^T \overline{R} K_1 \\ \phi_2 &= \lambda_2(k)(A(k) + BK_1)^T Q^{-1}(i+1,k)(A_d(k) \\ &\quad + BK_2) + K_1^T \overline{R} K_2 \\ \phi_3 &= \lambda_2(k)||A_d(k) + BK_2||_{K_d^{-1}(i+1,k)} \\ &\quad + K_2^T \overline{R} K_1 x(k+i-d|k) \\ \phi_4 &= \lambda_2(k)(A_d(k) + BK_2)^T K_d^{-1}(i+1,k)(A(k) \\ &\quad + BK_1) - K_d(i,k) + K_2^T \overline{R} K_2 \end{aligned}$$

By using Schur complement lemma, it can be transformed into the form of LMI as (29), shown at the bottom of the next page.

The Q, K_d of the matrix inequality is not unique, so it is impossible to determine the feedback matrix through the matrix. Therefore, the invertible matrices E_1 and E_2 are introduced to transform. The following linear matrix inequality

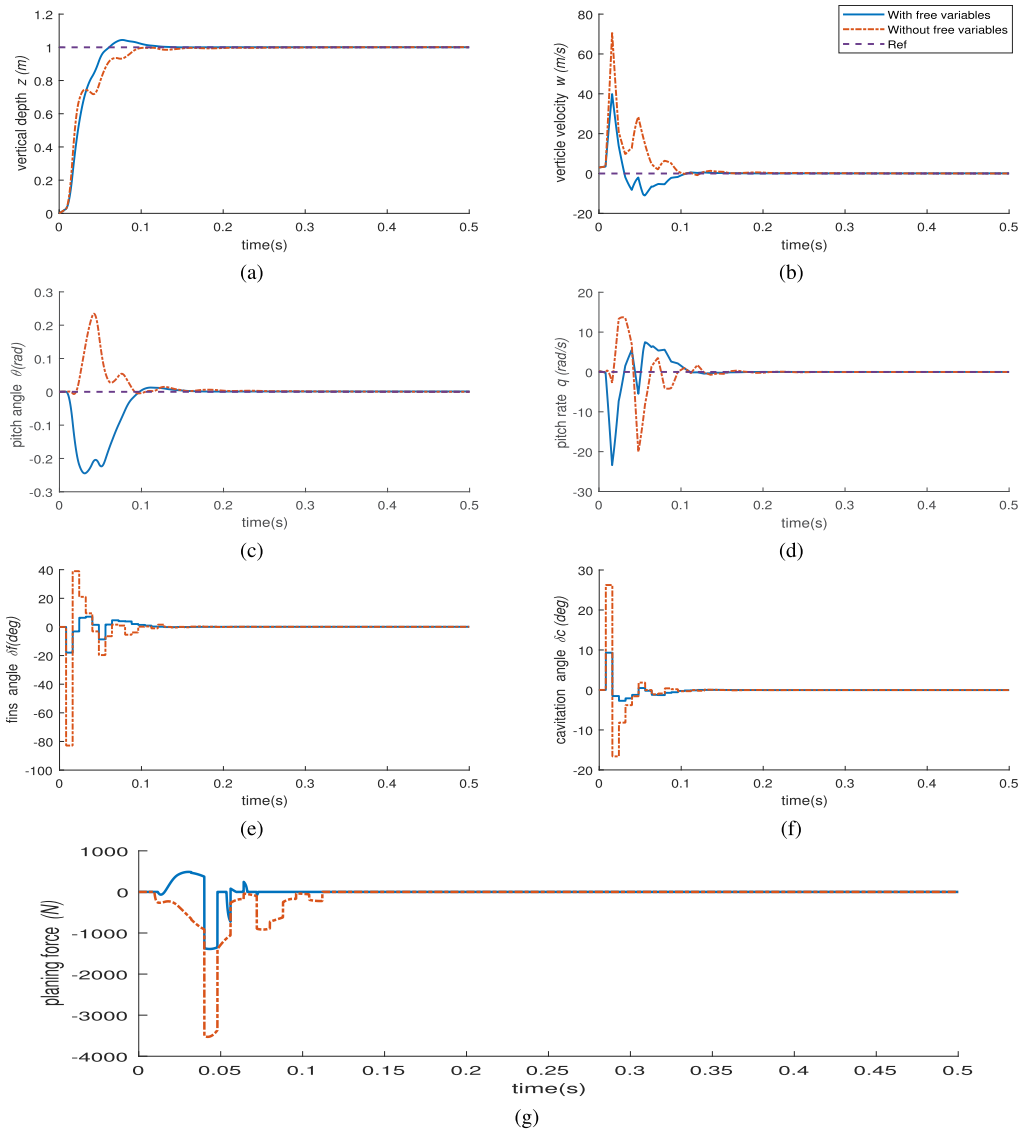

FIGURE 4. Step response curves of predictive control based on free control variables and predictive control.

can be obtained by making $Y_1 = K_1 E_1^{-1},\ Y_2 = K_2 E_2^{-1}$:

$$\begin{bmatrix} \Phi_1 & 0 & \Phi_2 & Y_1^T \overline{R}^{1/2} & E_1^T \overline{Q}^{1/2} & E_1^T \\ * & \Phi_3 & \Phi_4 & Y_2^T \overline{R}^{1/2} & 0 & 0 \\ * & * & Q_i & 0 & 0 & 0 \\ * & * & * & \lambda_2 I & 0 & 0 \\ * & * & * & * & \lambda_2 I & 0 \\ * & * & * & * & * & K_{di} \end{bmatrix} \geq 0 \quad (30)$$

where $i = 1 \ldots 4$.

$$\Phi_1 = E_1 + E_1^T - Q_i,\ \Phi_2 = (A_i E_1 + B Y_1)^T$$
$$\Phi_3 = E_2 + E_2^T - K_{di},\ \Phi_4 = (A_{di} E_2 + B Y_2)^T$$

□

After the above changes, the original min-max online optimization problem in the infinite time domain is finally

$$\begin{bmatrix} Q^{-1}(i,k) & 0 & (A(k) + BK_1)^T & K_1^T \overline{R}^{1/2} & \overline{Q}^{1/2} & I \\ * & K_d^{-1}(i+1,k) & (A_d(k) + BK_2)^T & K_2^T \overline{R}^{1/2} & 0 & 0 \\ * & * & Q(i+1,k) & 0 & 0 & 0 \\ * & * & * & \lambda_2 I & 0 & 0 \\ * & * & * & * & \lambda_2 I & 0 \\ * & * & * & * & * & K_d(i,k) \end{bmatrix} \geq 0 \quad (29)$$

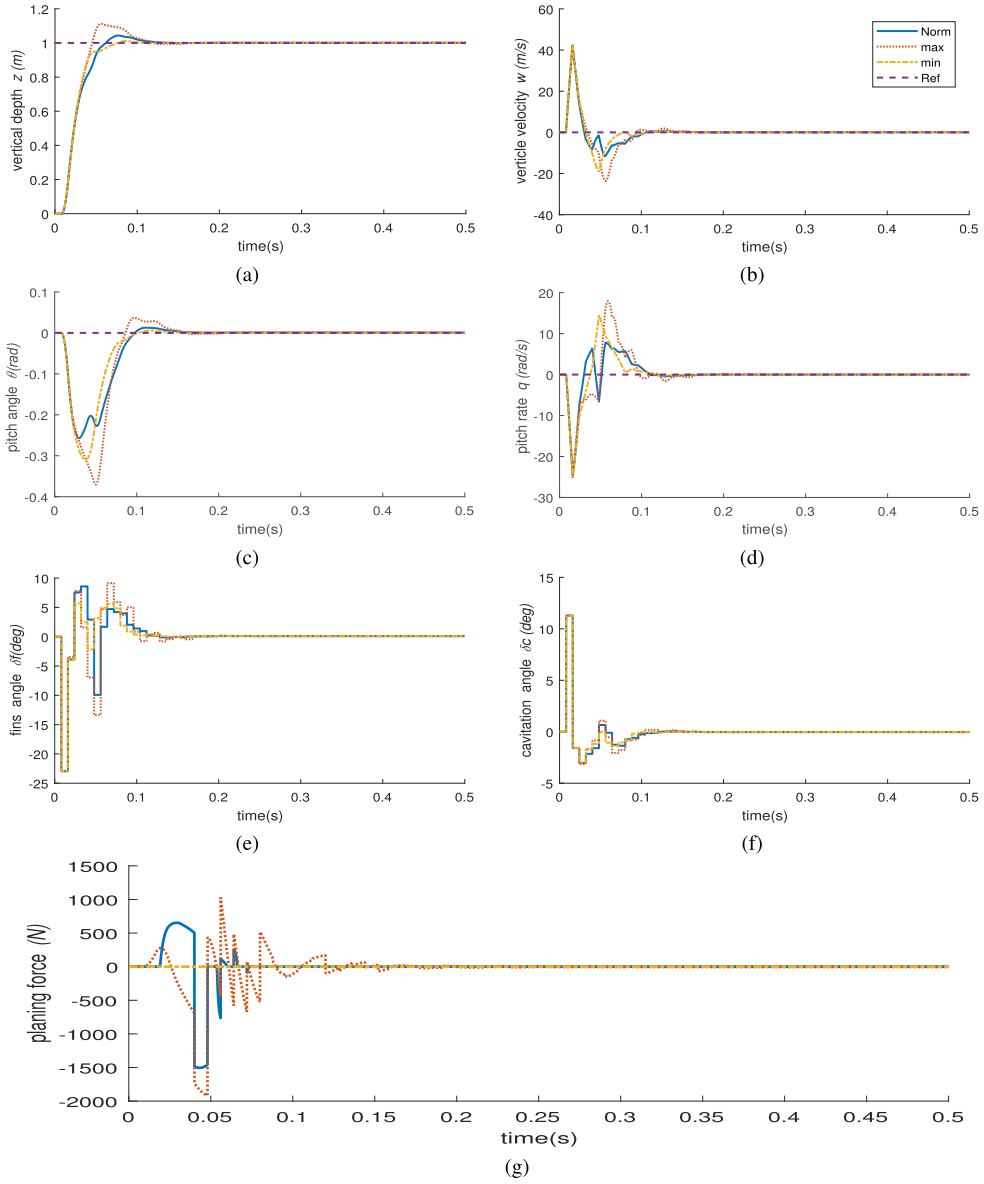

FIGURE 5. Step response curves of predictive control.

transformed into the following optimization problem:

$$\min_{U(k),E_1,E_2,Y_1,Y_2} \lambda_1 + \lambda_2 + ||x(k)||^2_Q$$
$$s.t\ (27),\ (28),\ (30) \tag{31}$$

where, the control variable at this sampling time is $u(k) = [I_{2\times 2}\ 0\ \ldots 0]U(k)$.

The algorithm designed in this section uses the time-varying Lyapunov function and introduces the free control variable into the infinite time domain based on the time-delay model of a supercavitating vehicle. The controller can guarantee the asymptotic stability of the system by terminal constraints. Meanwhile, free control variables can introduce the state of the system into a control invariant set in advance to expand the control invariant set of the system. Specifically, the system adopts a memory feedback control law for the present state and the time-delay state, which effectively accelerates the time of the system entering into the steady state.

IV. SIMULATION ANALYSIS

In this paper, aiming at the stability, robustness and tracking of the controller, we simulate and analyse the predictive controller designed in this paper. In this section, the delay time for the simulation is $\tau = L/V = 0.024s$. The sampling time of the system is set to $T = 0.008s$, and the prediction steps of the controller are set to $N = \tau/T = 3$. The reference signal of the system is set to $r = [z_r, w_r, \theta_r, q_r]^T$, then, the error signal of the system is $x_e = r - x$. The convex hull Ω of the system has 4 vertices $[A_i,\ A_{di}]$, $i = 1 \ldots 4$

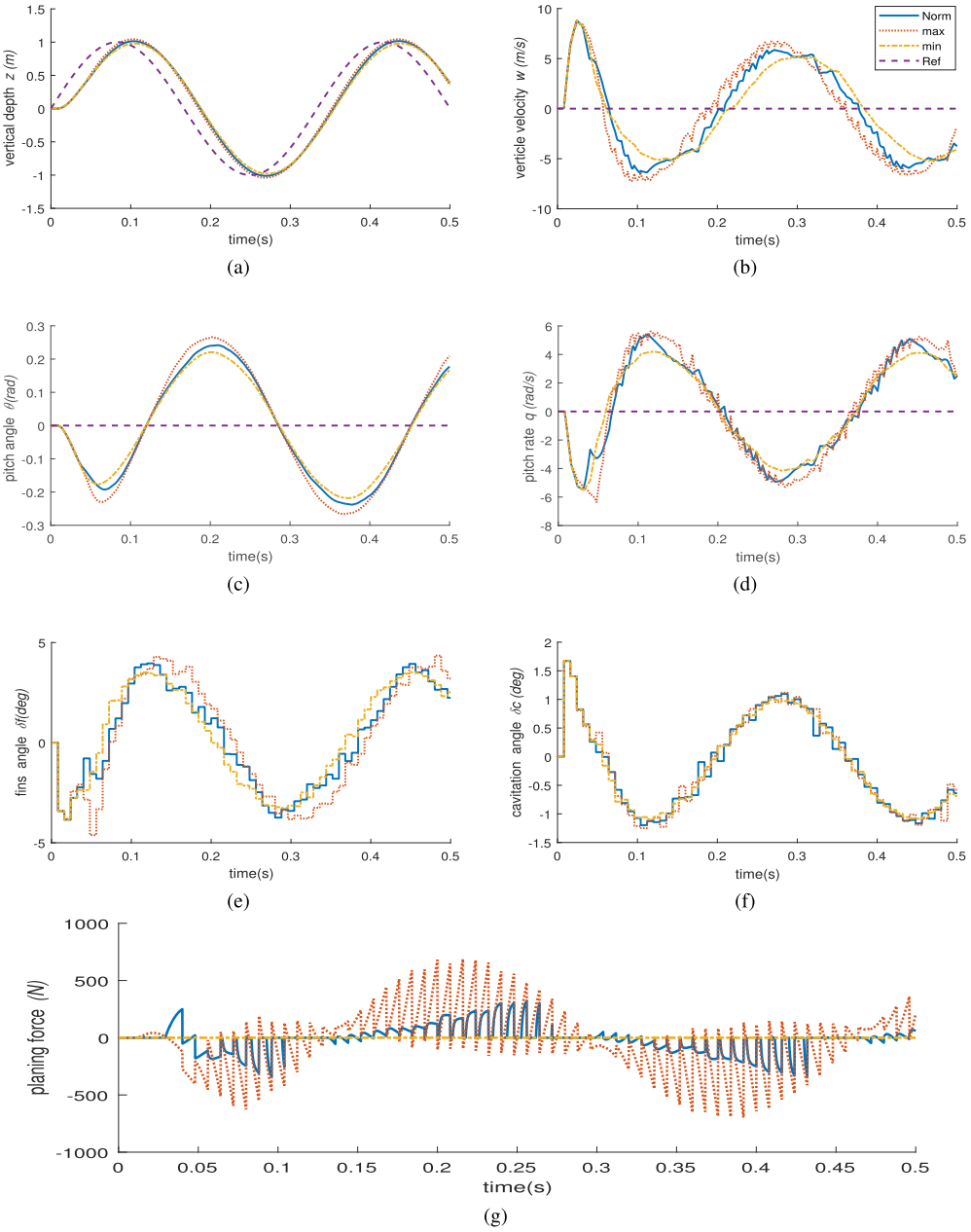

FIGURE 6. Sine tracking curves of predictive control.

because the system has two time-varying parameters π_1 and π_3. Therefore, the controller needs to solve 12 linear matrix inequalities online to obtain the optimal solution.

Fig. 4 shows the predictive control response curves with and without free control variables. The solid line shows the response of predictive controller designed in this paper. The dash-dotted line shows the response of the ordinary predictive controller without free control variables. The dashed line shows the reference signal $r = [1\ 0\ 0\ 0]^T$. It can be seen from Fig. 4 that the settling times of the two systems are similar. The controller with free control variables has a small overshoot, but the curve is relatively smooth. There is no overshoot from the ordinary predictive controller, but the depth curve fluctuates. In contrast, there is no significant difference between the two state responses. However, the controller designed in this paper has a smaller control variables, a smaller planing force and a shorter duration. Therefore, the controller designed in this paper has better control performance.

Fig. 5 shows the simulation curves of the predictive controller based on the free control variables of the supercavitating vehicle. The number of the free control variables is 2, $N = 3$. The solid line shows the response of the normal response curve of the system. The reference signal of the

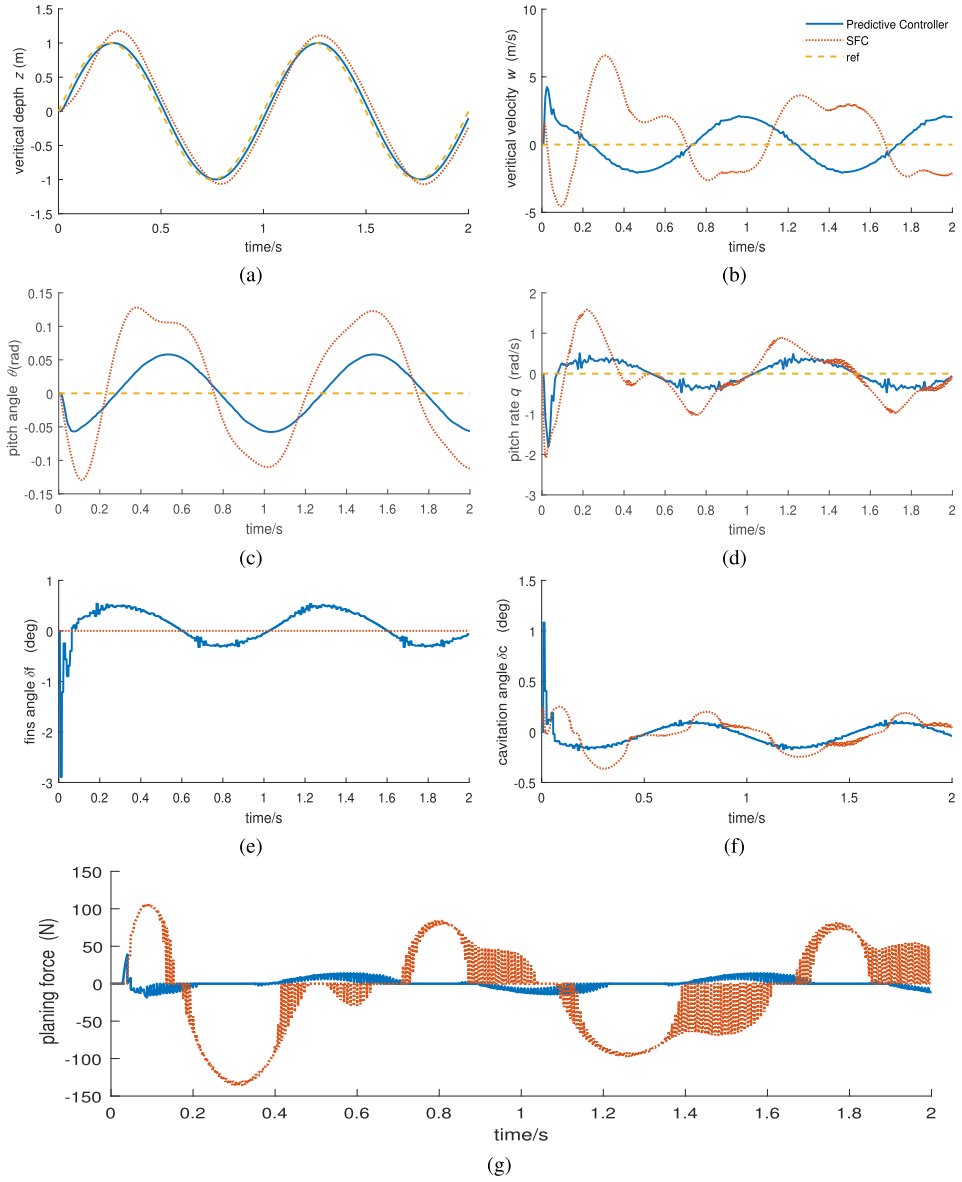

FIGURE 7. Sine tracking curves of the predictive controller and SFC.

system is $r = [1\ 0\ 0\ 0]^T$. The controller can follow the step signal of the depth to reach a stable value quickly, and the overshoot of the system is very small. The dotted line shows the response curve when the two parameters take the maximum value. At a given time, since the time-varying parameters are no longer zero, any change out of the stable state can produce a planing force. Therefore, the control difficulty of the system is greatly increased. The system exhibits a large overshoot, but it can reach a stable value quickly under the action of the controller. Therefore, the system has good robustness. The dash-dotted line shows the system response curve when the time-varying parameter takes the minimum value. At this moment, both π_1 and π_3 are zero, so the system has no time-delay and planing force. Meanwhile, the system settling time becomes larger, but it can still reach a stable state. After $N-1$ steps, the Lyapunov stability condition is introduced. The free control variables are introduced to expand the initial feasible region of the system. In addition, the influence of abnormal conditions on the system, such as minimax, is very small, and its response curve is close to the normal curve.

Fig. 6 shows the response curves of the system tracking sinusoidal signal. The depth of the reference signal is a sinusoidal signal $z = sin(6\pi t)$, and other state variables are zero $w = \theta = q = 0$. It can be seen in Fig. 6 that the system can effectively track the change in depth, and the maximum and minimum responses of the time-varying parameters are very close to the normal response curve of the system, which means that the system can still track the sinusoidal signal when the radius is perturbed by $\pm 20\%$. Fig. 7 shows the

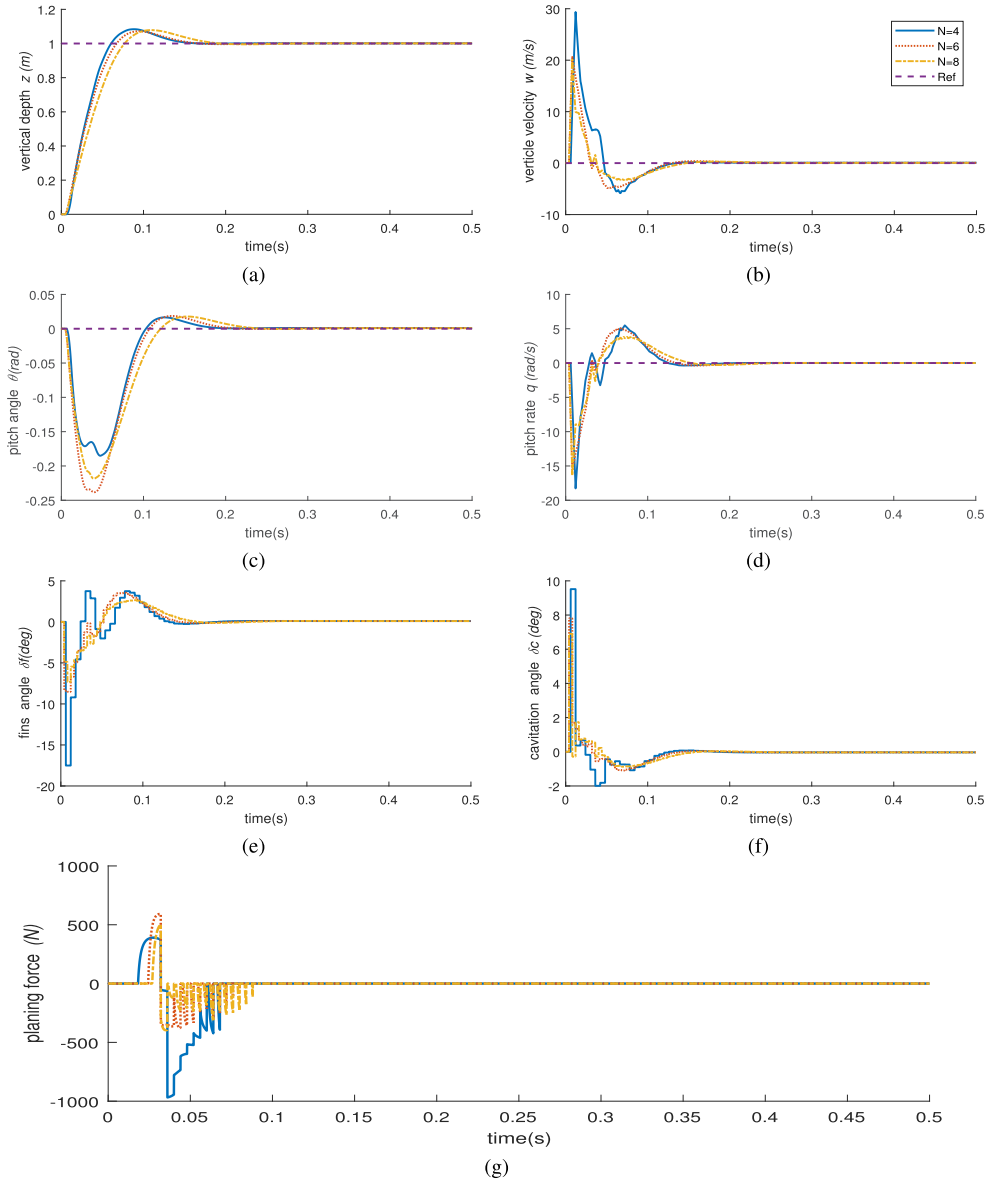

FIGURE 8. Predictive control curves of the vehicle with different free control variables.

response curves of the system tracking sinusoidal signal ($z = sin(2\pi t)$) for the predictive controller and the state feedback controller (SFC) [17]. We know that the depth curve of the predictive controller is closer to the reference signal than that of the SFC from Fig. 7. Therefore, the controller designed in this paper has strong tracking performance and robustness.

Fig. 8 shows the response curves of the predictive controller with different free control variables, in which the number of prediction steps are $N = 4$, $N = 6$ and $N = 8$. It can be seen from Tab. 2 that with the increase of prediction steps, the settling time of the system becomes longer, the overshoot of the system is basically unchanged, and the control variables of the system will decrease with the increase of free control variables. Meanwhile, the planing force of the system also decreases, but the number of times that the vehicle hits the cavitation wall increases.

TABLE 2. System performance index with different free control variables.

	N=4	N=6	N=8
settling time(s)	0.133	0.139	0.162
overshoot(%)	8.38	7.22	7.62
planing force(N)	968.5	588.7	498.6

V. CONCLUSION

In this paper, the time-delay model of a supercavitating vehicle was decomposed to establish an LPV time-delay model of a supercavitating vehicle. Considering the perturbation of cavitation radius, we designed a linear time-varying system of

supercavitating vehicle described by the polytope. Based on this model, a predictive controller with free control variables was designed. Meanwhile, several Lyapunov functions were used, which increases the degree of freedom in the design and improves the control performance of the system. Moreover, the controller added free control variables to transform the infinite time domain problem into a finite time domain problem with terminal constraints. The first $N-1$ free control variables can introduce the system state into the control invariant set, which expands the initial feasible region of the system. The terminal constraints can effectively guarantee the asymptotic stability of the system. In addition, the controllers were simulated when the time-varying parameter was maximum or minimum. it was shown that the controller exhibited good robustness and stability by simulation.

In the future, we plan to design a predictive controller with better control performance considering the parameters uncertainty, input delay, time-varying delay and actuator saturation of supercavitating vehicle to ensure that supercavitating vehicle can adapt to more complex working environment. Moreover, we will design the corresponding off-line algorithm to reduce the online workload of predictive control.

REFERENCES

[1] G. Logvinovich, "Hydrodynamics of flows with free boundaries," Naukova Dumka, Kyiv, Ukraine, Jan. 1969, p. 208.

[2] G. Logvinovich, "Some problems of planing surfaces," *Trudy TsAGI*, vol. 2052, pp. 3–12, Jan. 1980.

[3] B. Vanek, J. Bokor, and G. Balas, "Theoretical aspects of high-speed supercavitation vehicle control," in *Proc. Amer. Control Conf.*, Jun. 2006, p. 6.

[4] K. Luo, D.-J. Li, J.-J. Dang, Y.-C. Wang, and Y.-W. Zhang, "Motion control model of supercavitating vehicle considering time-delay effect of supercavitation," *Jiaotong Yunshu Gongcheng Xuebao*, vol. 10, no. 3, pp. 41–45, 2010.

[5] K. Luo, D.-J. Li, J.-J. Dang, Y.-C. Wang, and Y.-W. Zhang, "Nonlinear time delay kinematic model of underwater maneuverable supercavitating vehicles," in *Proc. 2nd Int. Conf. Intell. Hum.-Mach. Syst. Cybern.*, Aug. 2010, pp. 84–88.

[6] V. Nguyen and B. Balachandran, "Supercavitating vehicles with noncylindrical, nonsymmetric cavities: Dynamics and instabilities," *J. Comput. Nonlinear Dyn.*, vol. 6, no. 4, Oct. 2011, Art. no. 041001.

[7] V. Nguyen and B. Balachandran, "Supercavitating vehicle maneuvering with delay and non-steady planing," *Appl. Hydromech.*, vol. 15, no. 1, pp. 62–74, 2013.

[8] X.-H. Zhao, Y. Sun, G.-L. Zhao, and J.-L. Fan, "μ-synthesis robust controller design for the supercavitating vehicle based on the BTT strategy," *Ocean Eng.*, vol. 88, pp. 280–288, Sep. 2014.

[9] S. Kim and N. Kim, "Integrated dynamics modeling for supercavitating vehicle systems," *Int. J. Nav. Archit. Ocean Eng.*, vol. 7, no. 2, pp. 346–363, Mar. 2015.

[10] C. Huang, K. Luo, J. Dang, K. Qin, and D. Li, "Spatial kinetics model of supercavitating vehicles reflecting conic-like oscillation," *Math. Problems Eng.*, vol. 2017, pp. 1–12, Jan. 2017.

[11] B. Vanek, J. Bokor, and G. Balas, "High-speed supercavitation vehicle control," in *Proc. AIAA Guid., Navigat., Control Conf. Exhib.*, Aug. 2006, p. 6446.

[12] B. Vanek, G. J. Balas, and R. E. A. Arndt, "Linear, parameter-varying control of a supercavitating vehicle," *Control Eng. Pract.*, vol. 18, no. 9, pp. 1003–1012, Sep. 2010.

[13] R. Lv, K. Yu, Y. Wei, J. Zhang, and J. Wang, "Adaptive sliding mode controller design for a supercavitating vehicle," in *Proc. 3rd Int. Symp. Syst. Control Aeronaut. Astronaut.*, Jun. 2010, pp. 885–889.

[14] D. Escobar Sanabria, G. J. Balas, and R. E. A. Arndt, "Planing avoidance control for supercavitating vehicles," in *Proc. Amer. Control Conf.*, Jun. 2014, pp. 4979–4984.

[15] S. Kim and N. Kim, "Neural network-based adaptive control for a supercavitating vehicle in transition phase," *J. Mar. Sci. Technol.*, vol. 20, no. 3, pp. 454–466, Sep. 2015.

[16] X. Zhang, Y. Wei, Y. Han, T. Bai, and K. Ma, "Design and comparison of LQR and a novel robust backstepping controller for supercavitating vehicles," *Trans. Inst. Meas. Control*, vol. 39, no. 2, pp. 149–162, Feb. 2017.

[17] W. Deng, J. Yao, and D. Ma, "Time-varying input delay compensation for nonlinear systems with additive disturbance: An output feedback approach," *Int. J. Robust Nonlinear Control*, vol. 28, no. 1, pp. 31–52, Jan. 2018.

[18] J. Baek, S. Cho, and S. Han, "Practical time-delay control with adaptive gains for trajectory tracking of robot manipulators," *IEEE Trans. Ind. Electron.*, vol. 65, no. 7, pp. 5682–5692, Jul. 2018.

[19] M. A. Hassouneh, B. Balachandran, and E. H. Abed, "Delay effects in supercavitating vehicle dynamics," in *Proc. ASME Int. Design Eng. Tech. Conf. Comput. Inf. Eng. Conf.*, San Diego, CA, USA: American Society of Mechanical Engineers Digital Collection, 2009, pp. 653–660.

[20] M. A. Hassouneh, V. Nguyen, B. Balachandran, and E. H. Abed, "Stability analysis and control of supercavitating vehicles with advection delay," *J. Comput. Nonlinear Dyn.*, vol. 8, no. 2, Apr. 2013, Art. no. 021003.

[21] B. Vanek, J. Bokor, G. J. Balas, and R. E. A. Arndt, "Longitudinal motion control of a high-speed supercavitation vehicle," *J. Vibrat. Control*, vol. 13, no. 2, pp. 159–184, Feb. 2007.

[22] X. Jin, G. Yin, X. Zeng, and J. Chen, "Robust gain-scheduled output feedback yaw stability control for in-wheel-motor-driven electric vehicles with external yaw-moment," *J. Franklin Inst.*, vol. 355, no. 18, pp. 9271–9297, Dec. 2018.

[23] X. Mao and Q. Wang, "Robust control of time-delay systems with application to a supercavitating vehicle," in *Proc. ASME Dyn. Syst. Control Conf., A B*, Jan. 2008, pp. 907–914.

[24] V. Nguyen, M. A. Hassouneh, B. Balachandran, and E. H. Abed, "Non-steady planing and advection delay effects on the dynamics and control of supercavitating vehicles," in *Proc. Dyn. Syst. Control; Mechatronics Intell. Mach., A B*, vol. 7, Jan. 2011, pp. 775–781.

[25] X. Zhao, G. Duan, and Y. Sun, "Complex control system design for time delay supercavitating vehicle," *Eng. Mech.*, vol. 28, no. 9, pp. 234–239, 2011.

[26] M. Lin, M. Xiang, W. Zhang, and X. Yang, "Fast trajectory optimization for the time delay effect on supercavitating flight," *Brodogradnja, Teorija i Praksa Brodogradnje i Pomorske Tehnike*, vol. 63, no. 3, pp. 219–225, 2012.

[27] L. Xiong, H. Li, and J. Wang, "LMI based robust load frequency control for time delayed power system via delay margin estimation," *Int. J. Electr. Power Energy Syst.*, vol. 100, pp. 91–103, Sep. 2018.

[28] Y.-G. Sun, S. Xie, J.-Q. Xu, and G.-B. Lin, "A robust levitation control of maglev vehicles subject to time delay and disturbances: Design and hardware experimentation," *Appl. Sci.*, vol. 10, no. 3, p. 1179, Feb. 2020.

[29] X. Mao and Q. Wang, "Delay-dependent control design for a time-delay supercavitating vehicle model," *J. Vibrat. Control*, vol. 17, no. 3, pp. 431–448, Mar. 2011.

[30] D. Li, K. Luo, C. Huang, J. Dang, and Y. Zhang, "Dynamics model and control of high-speed supercavitating vehicles incorporated with time-delay," *Int. J. Nonlinear Sci. Numer. Simul.*, vol. 15, nos. 3–4, pp. 221–230, Jan. 2014.

[31] J. Dong, Y. Wu, and G. H. Yang, "A new sensor fault isolation method for t–s fuzzy systems," *IEEE Trans. Cybern.*, vol. PP, no. 9, pp. 1–11, 2017.

[32] B. D. H. Phuc, V.-D. Phung, S.-S. You, and T. D. Do, "Fractional-order sliding mode control synthesis of supercavitating underwater vehicles," *J. Vibrat. Control*, vol. 26, nos. 21–22, pp. 1909–1919, Nov. 2020.

[33] X. Feng, H. Hu, M. E. Villanueva, and B. Houska, "Min-max differential inequalities for polytopic tube mpc," in *Proc. Amer. Control Conf. (ACC)*. Philadelphia, PA, USA: IEEE, 2019, pp. 1170–1174.

[34] Q. Weiwei, L. Jieyu, H. Xiaoxiang, H. Bing, and L. Gang, "Tube-based active robust MPC for uncertain constrained linear systems with time delays," *IEEE Access*, vol. 7, pp. 125552–125561, 2019.

[35] F. A. Cuzzola, J. C. Geromel, and M. Morari, "An improved approach for constrained robust model predictive control," *Automatica*, vol. 38, no. 7, pp. 1183–1189, Jul. 2002.

YUNTAO HAN received the M.Sc. and Ph.D. degrees in control science and engineering from Harbin Engineering University (HEU), Harbin, China, in 2007 and 2009, respectively. From November 2017 to November 2018, he was a Visiting Researcher with Bauman Moscow State Technical University. He is currently a Lecturer with the College of Intelligent Systems Science and Engineering, Harbin Engineering University. He is the author of three books, more than 30 articles, and five invention patents. His research interests include dynamic modeling and control of underwater high-speed vehicle, path planning of underwater robot, embedded systems.

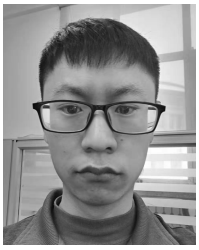

ZHEN XU was born in Zibo, Shandong, China, in 1995. He received the B.E. degree in automation from the Qingdao University of Science and Technology, in 2018. He is currently pursuing the M.Sc. degree with the Department of Control Science and Engineering, Harbin Engineering University. His research interest includes control of underwater high-speed vehicle.

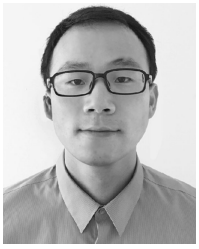

LIANWU GUAN received the B.Sc. degree in M&C technology and instrumentation, in 2011, the M.Sc. degree, and the Ph.D. degree in navigation, guidance and control from Harbin Engineering University (HEU), Harbin, China, in 2016. From September 2014 to March 2016, he was a Visiting Researcher with the Department of Electrical and Computer Engineering, Queen's University, and Royal Military College of Canada in Kingston, Canada. Since 2017, he has been a Postdoctoral Researcher with the College of Intelligent Systems Science and Engineering, HEU, where he is currently a Lecturer. He is the author or coauthor over 25 scientific articles and over 20 patents in China, USA, Japan, France, and other countries. His research interests include inertial measurement unit (IMU), inertial-based integrated navigation and localization systems with their application in pipeline inspection and localization robots, intelligent ski machine, unmanned autonomous vehicle, underwater autonomous vehicle, and other fields.